Quasi-phase-matched second-harmonic generation in Ge-ion implanted fused silica channel waveguide

Shiuh Chao[1], Huai-Yi Chen[2], Yu-HsienYang[1], Ze-Wen Wang[1], Chih T'sung Shih[3] and Huan Niu[4]

[1]Institute of Photonics Technologies, National Tsing Hua University, HsinChu 30055, Taiwan, R.O.C.
schao@ee.nthu.edu.tw
[2]Department of Electronic Engineering, Huafan University, Taipei 223, Taiwan, R.O.C..
[3]Opto-Electronics & Systems Laboratories, Industrial Technology Research Institute, HsinChu 310, Taiwan, ROC.
[4]Nuclear Science and Technology Development Center, National Tsing Hua University, HsinChu 30055, Taiwan, ROC.

Abstract: Channel waveguides were formed on fused silica substrate by Ge-ion implantation with lithographically defined channels. Thermal poling was performed to form second order optical nonlinearity (SON) in the waveguides. Periodical photo masks were designed and fabricated on a mask glass. Periodical erasure of the SON in the channel waveguides by 266 nm UV light with the photo mask on the fused silica substrate produced periodical SON distribution in the waveguides. First order quasi-phase-matching second-harmonic generation from 1064 nm to 532 nm was demonstrated in the channel waveguides.

OCIS Codes: (190.2620) Frequency conversion; (190.4400) Nonlinear optics, materials; (190.4360) Nonlinear optics, devices

Reference and links

1. R.A. Myers, N. Mukherjee, and S.R.J. Brueck, "Large second-order nonlinearity in poled fused silica," Opt. Lett. **16**, 1732-1734 (1991).
2. R. H. Stolen and H. W. K. Tom, "Self-organized phase-matched harmonic generation in optical fibers,"Opt. Lett. **12**, 585-587 (1987).
3. V. Pruneri, F. Samoggia, G. Bonfrate, P. G. Kazansky, and G. M. Yang, "Thermal poling of silica in air and under vacuum: The influence of charge transport on second harmonic generation," Appl. Phys. Lett. **74**, 2423-2425 (1999).
4. W. Margulis and F. Laurell, "Interferometric study of poled glass under etching,"Opt. Lett. **21**, 1786-1788 (1996).
5. A.L.C. Triques, I.C.S. Carvalho, M.F. Moreira, H.R. Carvalho, R. Fischer, B. Lesche, and W. Margulis, " Time evolution of depletion region in poled silica," Appl. Phys. Lett. **82**, 2948-2950 (2003).
6. F. C. Garcia, L. Vogelaar, and R. Kashyap, "Poling of a channel waveguide," Opt. Express **11**, 3041-3047 (2003).
7. A. C. Liu, M. J. F. Digonnet and G. S. Kino, "Electro-optic phase modulation in silica channel waveguide," Opt.Lett. **19**, 466-468 (1994).
8. H.Y. Chen, C.L.Lin, Y.H. Yang, S.Chao, H.Niu, and C.T.Shih, "Creation of second-order nonlinearity and quasi-phase-matched second harmonic generation in Ge-implanted fused silica planar waveguide," Appl. Phys. Lett. **86**, 081107 (2005).
9. J. F. Ziegler, J. P. Biersack, and U. Littmark, The Stopping and Range of Ions in Solids, (Pergamon, New York, 1985).
10. H. Y. Chen, J. S. Sue, Y.H. Lin, C. S. Tsai, P. T. Wu, and S. Chao " Thermal poling and ultraviolet erasure characteristics of type-III ultraviolet-grade fused silica and application to periodic poling on planar substrates" J. Appl. Phys. **94**, 1531-1538 (2003).
11. M. M. Fejer, G. A. Magel, D. H. Jundt, and R. L. Byer, "Quasi-phase-matched second harmonic generation: tuning and tolerances ," IEEE J. Quantum Electron. **28**, 2631-2654 (1992).

#8201 - $15.00 USD Received 18 July 2005; revised 27 August 2005; accepted 28 August 2005

1. Introduction

In glassy material, the macroscopic central-symmetrical structure prohibits the existence of the second order optical nonlinearity (SON). In 1991, Myers *et al* found that SON could be created in fused silica plate by thermal poling [1]. Creating a built-in DC electric field near the anodic surface through thermal poling and coupling of this field with the third order nonlinearity to form the SON, i.e. $\chi^{(2)} \sim \chi^{(3)} E_{dc}$, was believed to be one of the possible mechanisms for SON formation in thermally poled glass material[1,2]. Since the SON only forms in the shallow region close to the anodic surface[1],[3-5], it will be more useful, in practical devices, to form waveguide with SON at the anodic surface[6,7]. Our previous paper[8] reported results on thermal poling and quasi-phase-matching second-harmonic generation (QPM-SHG) in Ge-implanted silica planar waveguide with formation of periodic SON by periodic UV erasure of SON in the waveguide. In this paper, we extended the technique to form Ge-implanted silica channel waveguides and demonstrated QPM-SHG of 1064nm to 532 nm in the channel waveguides.

2. Device design and fabrication

Multiple parallel channel waveguides were fabricated according to the procedure depicted in Fig. 1. A 3 μm thick aluminum layer was deposited on the 14 mm × 14 mm type-I fused silica plate (GE124) by electron beam evaporation, followed by depositing a spin-coated photo resist layer. Multiple parallel channels, 30 μm apart, 4 μm in width for each channel were formed on the photo resist layer by UV exposure and wet etching. Reactive Ion Etching (RIE) was used to dry-etch the aluminum layer and opened the channel pattern on the fused silica for the following ion implantation process. Ion implantation was performed on a National Electrostatics Corp. 9SDH-2 tandem accelerator. Ge^{+2} ion beam with 5 MeV energy and 1×10^{15} cm^{-2} ion dose was generated for implantation. The implantation time was about 100 minutes, the implanted area on the sample was 14 mm × 14 mm, and the total ion count, i.e. number of Ge^{+2} ion impinging the fused silica surface, was therefore about 8 million. The backside of the fused silica substrate was attached to a copper plate and cooled with liquid nitrogen during implantation. The ion distribution in the fused silica along the direction of the depth, under our implantation condition, was Gaussian-like with the peak located at 2.9 μm from the surface and the FWHM of the Ge-ion distribution was ~0.9 μm as was calculated with the software of SRIM [9], the waveguide was therefore buried beneath the fused silica surface.

Figure 2(a) shows the optical microscope top-view of the sample after RIE dry-etching process. The bottom of the channel was 4 μm wide with a graduate rising edge of the aluminum film. Therefore, the subsequent ion implantation would not produce an exact 4 μm wide laterally uniform channel waveguide in the substrate; rather the ion distribution would be a chevron-like shape. With the aid of SRIM software, we have calculated the ion distribution beneath the areas that was covered by different thickness of aluminum. The dash line in Fig. 2(b) represents the peak location of the Gaussian-like Ge profile. We then assume that the refractive index of the waveguide material is directly proportional to Ge concentration; the peak change of the refractive index, Δn, could be obtained according to the method introduced in the next paragraph, the refractive index distribution of the channel waveguide could therefore be obtained. Software of Beam-Propagation-Method (BPM) was then used to calculate the effective index of the waveguide mode and mode profile. A typical chevron-like shape fundamental mode profile is shown in Fig. 2(c).

#8201 - $15.00 USD Received 18 July 2005; revised 27 August 2005; accepted 28 August 2005

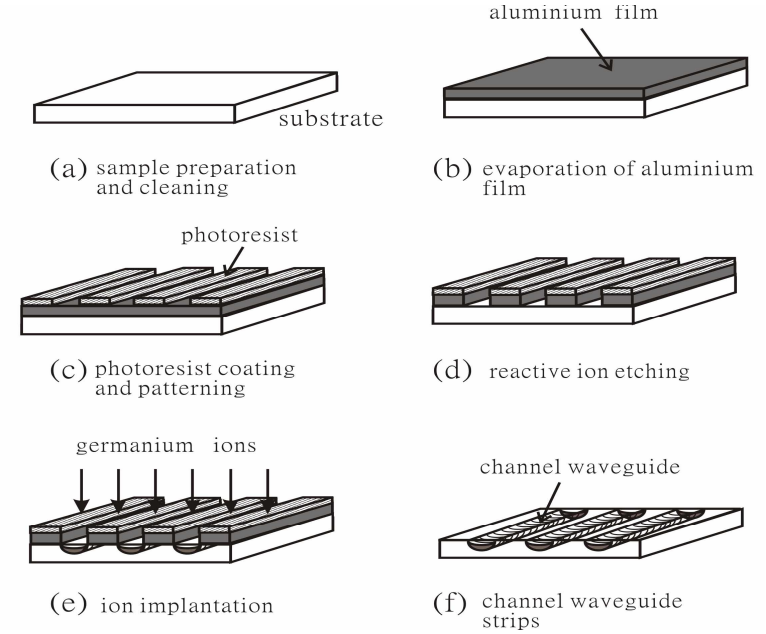

Fig. 1. Fabrication flow of multiple channel waveguides.

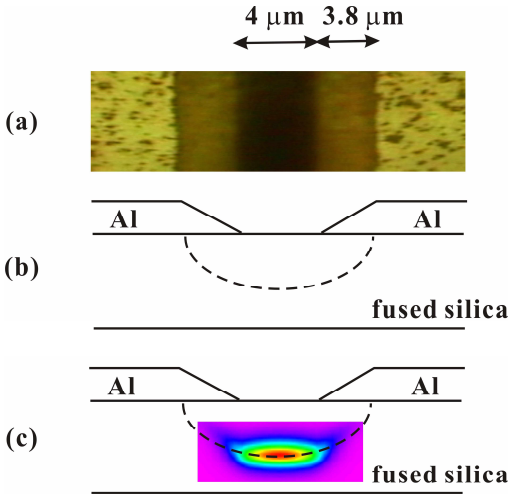

Fig. 2. (a) Top-view of the sample under optical microscope after dry etching. (b) Schematic cross-section view of the ion-implanted sample. Dash line is the peak location of the Gaussian-like germanium profile. (c) Simulated chevron-like shape mode pattern.

For purpose of QPM-SHG from 1064 nm to 532 nm in the channel waveguide, we need to know, experimentally, the mode effective index for both wavelengths in order to calculate the correct period for the first order QPM in the channel waveguide according to the equation:

$$\Lambda = \frac{\lambda_{\omega}}{2(N_{2\omega} - N_{\omega})} \tag{1}$$

#8201 - $15.00 USD Received 18 July 2005; revised 27 August 2005; accepted 28 August 2005

where λ_ω is the fundamental wavelength, $N_{2\omega}$ and N_ω are mode effective indices of second harmonic and fundamental waves, respectively.

The procedure for estimating the periodicity of the first order QPM in the channel waveguide was done as follows: We used prism coupler, which was equipped with three wavelengths: 1547 nm, 1308 nm and 633 nm respectively, to measure the mode effective index of the planar waveguide at these wavelengths. The planar waveguide was fabricated identically to the channel ones but without lithographic process. Assuming that the refractive index of the waveguide material is directly proportional to the ion concentration, by using SRIM and BPM software, we adjusted the peak refractive index of the Gaussian-like index profile such that the calculated mode index equals to the measured mode index for these three wavelengths. The difference between the peak refractive index of the waveguide and the fused silica substrate,Δ n, versus wavelength is shown in Fig. 3. The peak refractive index of the Gaussian-like profile for 1064 nm and 532 nm wavelength could therefore be interpolated and extrapolated from Fig.3, and these data were then put into the BPM software to obtain the mode effective index of the chevron-like shape channel waveguide mode for 1064 nm and 532 nm wavelength. Once the mode effective indices were known, the period of first order QPM-SHG for 1064 nm to 532 nm conversions could be obtained from Eq. (1). The period was estimated to be ~33 μm for s to s and p to s conversions.

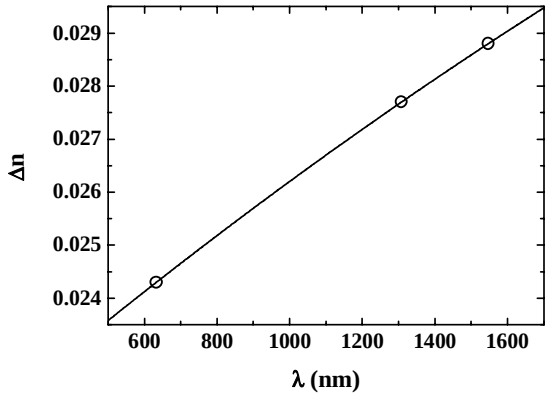

Fig. 3. Difference between the peak refractive index of the waveguide and the substrate as a function of wavelength.

The procedure described above involving certain degree of uncertainty, however, the value so obtained provided a good starting point to figure out the exact period. In order to catch the exact period for quasi-phase-matching on the sample, we produced multiple parallel channel waveguides on a single fused silica plate; the fabrication method was introduced previously. The multiple channel waveguides were identical; each channel was separated 30 μm apart. Thermal poling at 275°C and 6kV for 15 minutes was performed on the whole substrate with anode on the waveguide side to create second order optical nonlinearity in the waveguides. Series of photo masks 30 μm in separation on a single mask glass was prepared. Each mask composed of ~ 41% duty periodical aluminum strip. The periodicity of the aluminum stripe varied from mask to mask with 0.1 μm increments. Each mask covered one channel waveguide when the mask glass was in contact with the substrate. The 266 nm UV light with 4~6 ns pulse width and 8mJ pulse power from a frequency quadrupled Nd-YAG laser (Spectra-Physics Quanta-Ray INDI-50) was used to illuminate the substrate through the masks. Second order optical nonlinearity of the area that was not covered by the mask in the

#8201 - $15.00 USD Received 18 July 2005; revised 27 August 2005; accepted 28 August 2005

waveguide could be erased when exposed to the UV light [8,10]. Periodical second order optical nonlinearity along the channel waveguide was therefore produced, the periodicity increased in 0.1 μm step from channel to channel.

3. Experimental results

SHG test was performed on each waveguide in sequence; each waveguide has QPM periodicity that was 0.1 μm differed to the adjacent waveguide 30 μm apart. Fig. 4(a) and (b) showed the SHG signal strength for s to s polarization conversion and p to s polarization conversion for each waveguide, plotted as $P_{2\omega}$ vs. $1/\Lambda$. Solid lines in Fig. 4 are sinc^2 functions fitted to the experimental points according to the equation:

$$P_{2\omega} = \frac{8\pi^2 d_{Q,eff}^2 L^2}{N_\omega^2 N_{2\omega} c\varepsilon_0 \lambda_\omega^2} \frac{P_\omega^2}{A_{OVL}} \sin c^2 \left(\Delta\beta L/2\right) \quad (2)$$

where $d_{Q,eff}$ is the effective second-order nonlinear coefficient and L is interaction length, mismatching factor $\Delta\beta$ is defined as $\beta_{2\omega} - 2\beta_\omega - 2\pi/\Lambda$, β is mode propagation constant, c and ε_0 are individually light speed and permittivity in vacuum, and A_{ovl} is equivalent overlap area .

Insets of Fig. 4(a) and (b) showed the observed SH mode pattern for the highest SH output power waveguides. Fig. 5 and the inset showed the SH output power variation with the 1064 nm input power for the channel waveguides which have the highest SH output power in Fig. 4(a) and (b), respectively. The characteristic parabolic SHG curves are clearly shown in Fig. 5. We can estimate $d_{Q,eff}$ by substituting the peak value of $P_{2\omega}$ from Fig. 4(a) and (b), the experimental value of P_ω, the calculated values of N_ω, $N_{2\omega}$, and A_{ovl} into Eq. (2). We found that $d_{Q,eff}$ equals to 0.03 pm/V and 0.006 pm/V for s-s and p-s conversions, respectively. Notice that, these values are QPM-dependent, and due to the non-uniform Ge-distribution, they are likely to be mode-dependent.

Waveguide coupling coefficient in our SHG test setup for coupling the 1064 nm light into the waveguide can be estimated by taking the ratio of the input and output power of the non-phase-matched waveguide. Taking the ratio of the 1064 nm input power to the 532 nm output power of the phase-matched waveguide with the known coupling coefficient of 1064 nm light, we could obtain the SHG conversion efficiency. These estimations were based on the assumption that absorption and scattering loss of 1064 nm and 532 nm light in our channel waveguides were negligible. For the s to s polarization conversion of the 34 μm period waveguide that has the highest SH output power in Fig. 4(a), we obtained second-harmonic peak power of ~1.8 μW with fundamental peak pumping power of ~780 mW, the SH conversion efficiency was 6.1×10^{-4} %/W-cm^2. The length of our channel waveguides was 7 mm. As compared with our previous QPM-SHG result in the planar waveguide [8], the SH conversion efficiency was improved by about three orders of magnitude for the channel waveguide. We estimated, by theoretically calculating the waveguide mode patterns and overlap integrals with known refractive index distribution for both planar and channel waveguides, that the overlap integral improved a factor of ~560 with channel waveguide. Taking this factor together with the measured conversion efficiency and considering the effect of the differences in duty cycles of the QPM period [11], we found from Eq.(2) that d_{Qeff} improved by a factor of ~6.4 for the channel waveguide. Since we used type III KU fused silica substrate for planar waveguide and type I GE124 fused silica substrate for channel waveguide, the improvement in the d_{Qeff} should therefore be related to the differences in the substrate material and UV erasure mechanisms in the different substrate materials. Further

#8201 - $15.00 USD Received 18 July 2005; revised 27 August 2005; accepted 28 August 2005

studies on these aspects need to be carried out in order to understand the causes for the material improvement.

4. Conclusion

In conclusion, second order optical nonlinearity was created in Ge-ion-implanted channel waveguides on fused silica substrate with thermal poling; periodic second order optical nonlinearity distribution in the channel waveguides was achieved by periodic UV erasure of the second order optical nonlinearity. First order QPM-SHG was demonstrated in the channel waveguides.

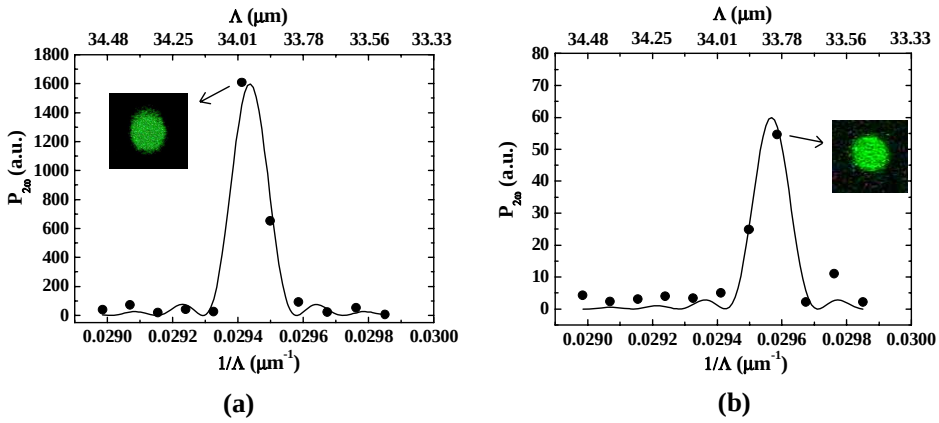

Fig. 4. Dependence of SH signal on inverse period, 1/Λ , for (a) s to s and (b) p to s conversions in each waveguide. Insets: SH mode pattern observed for the highest SH output power channel waveguide.

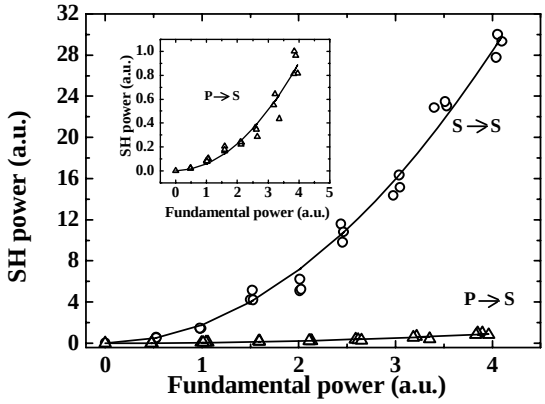

Fig. 5. The relation between second harmonic and fundamental powers for s to s (open circles) and p to s (open triangles) conversions. Solid lines are theoretically fitted parabolic curves.

#8201 - $15.00 USD Received 18 July 2005; revised 27 August 2005; accepted 28 August 2005